A Land Surface Model (IAP94) for Climate Studies Part I: Formulation and Validation in Off-line Experiments①

Dai Yongjiu (戴永久) and *Zeng Qingcun* (曾庆存)
Institute of Atmospheric Physics, Chinese Academy of Sciences, Beijing 100080
Received May 14, 1997

ABSTRACT

The IAP (Institute of Atmospheric Physics) land-surface model (IAP94) is described. This model is a comprehensive one with detailed description for the processes of vegetation, snow and soil. Particular attention has been paid to the cases with three water phases in the surface media.

On the basis of the mixture theory and the theory of fluid dynamics of porous media, the system of universal conservational equations for water and heat of soil, snow and vegetation canopy has been constructed. On this background, all important factors that may affect the water and heat balance in media can be considered naturally, and each factor and term possess distinct physical meaning. In the computation of water content and temperature, the water phase change and the heat transportation by water flow are taken into account. Moreover, particular attention has been given to the water vapor diffusion in soil for arid or semi-arid cases, and snow compaction. In the treatment of surface turbulent fluxes, the difference between aerodynamic and thermal roughness is taken into account. The aerodynamic roughness of vegetation is calculated as a function of canopy density, height and zero-plane displacement. An extrapolation of log-linear and exponential relationship is used when calculating the wind profile within canopy.

The model has been validated against field measurements in off-line simulations. The desirable model's performance leads to the conclusion that the IAP94 is able to reproduce the main physical mechanisms governing the energy and water balances in the global land surface. Part II of the present study will concern the validation in a 3-D experiment coupled with the IAP Two-Level AGCM.

Key words: Land Surface Model, Off-line Experiment, Validation

I. INTRODUCTION

In recent years, parallel to the proliferation of climate change studies using AGCMs, many land-surface parameterization schemes (LSPs) have been proposed, which range from rather simple to complex representations of soil and vegetation. Most of them have been applied to AGCM following limited off-line calibrating and testing, and have shown the improvement of the representation of surface climates. Simulations of surface climate by AGCM are not only sensitive to the changes of the surface albedo, roughness, soil moisture, and evapotranspiration, but also very much dependent on the formulation of their LSPs (see the review of Garratt, 1993; Sellers et al., 1996). Increased realism in the climate modelling has been shown that the improvement of the land surface component of coupled climate models is still a challenging task (Gates et al., 1996).

①This work was funded by the National Key Project of Fundamental Research "Climate Dynamics and Climate Prediction Theory" of China.

The global landscape can be simply classified into three major types: vegetation cover, desert and the permanent or seasonal snow. There exist great differences in energy and water partitioning at the surface of these media due to the differences of their thermal and hydrological characteristics. Current schemes are concentrated mainly on soil and vegetation processes incorporating with only some rudimentary considerations on snow, desert and frozen soil (Dickinson et al., 1993; Sellers et al., 1996, etc.). One of the challenges in developing LSP using in AGCMs is how to comprise a comprehensive and accurate description for all these different surface types without overwhelming the parent model with its computational requirements.

One of the difficulties in establishing a comprehensive LSP may be the presentation of universal control equations of temperature and water for all kinds of surface media. In dealing with this problem, it is unavoidable to have variable coefficients in diffusive equations. A series of experimental studies have shown that the specific heat capacity of frozen soil is about half of that of unfrozen soil at the same water content (including ice), which undergoes a sudden change about 0 C, and is largely dependent on the water content; while the heat conductivity is less dependent on the temperature change, but largely dependent on the water content (Haynes et al., 1980). Thus, if we study the mixture cases in which snow, frozen soil or unfrozen soil coexist, we must treat the variable coefficient diffusive problems. Regarding the calculation of ground temperature, generally, two main types are used in the present LSPs: one is the force–restore method, and the other is the direct spatial discretization of the thermal diffusive equation. The former, which is derived from the assumptions of periodic heating and uniform thermal properties (Bhumralkar, 1975), requires considerable modification if inhomogeneous or snow covered soils are concerned (Dickinson, 1988). As for the latter, if explicit method is adopted, in order to avoid the computational error and instability, a harsh relationship between the time interval and spatial thickness must be satisfied; while, if implicit method is adopted, it is generally CPU consumption. Since its physical meaning is clear in comparison with force–restore method, it is still used in some of LSPs (Verseghy, 1991; Viterbo and Beljaars, 1995, etc.). In the direct discretization method case, in order to apply a large thickness of ground surface layer, a zero heat capacity skin layer for surface is usually introduced. Nevertheless it can not evade the embarrassment of the nonconservation and the overestimated evaporation in drying period. The same criticisms can be made also for the moisture calculations.

A new LSP, suitable for various land surface media, has been developed in order to tackle the problems referred above. Special attention has been devoted to an accurate representation of the control equations for energy and moisture. In the natural environment, soil, snowpack or vegetation canopy are a complex assembly of solid matrix, three phases of water and dry air. Morland et al. (1990) had laid down a rigorous theoretical framework for a four constituents phase–changing snowpack, which were derived from the principles of mixture theory. A simplified one–dimensional approach has been successfully used for snow cover by Jordan (1991). In addition, there are many works on fluid dynamics for porous media in engineering and water resource (Bear, 1972). In the viewpoint of the mixture theory and the fluid dynamics in porous media, we try to develop a set of universal control equations of energy and water for the global land surface media. In the model development, we also attempt to improve the calculation of the surface radiation fluxes and turbulent fluxes between surface and the atmosphere. In the numerical solution, the control–volume approach of Patankar

(1980) is adopted for the spatial discretization, which leads itself to direct physical interpretation, and quantity conservation over control volumes rather than at an infinitesimal point as with a finite-difference scheme. As the time discretization procedure, Crank-Nicolson method is used. Governing set of equations are linearized with respect to the unknown variables and solved by the tridiagonal-matrix algorithm.

The next section of this paper introduces the conservation equations for global land surface media. In Sections 3, the parameterizations for the water flow within vegetation canopy, soil and snow are given. Sections 4 and 5 present the parameterization scheme of the radiation flux and the heat and moisture fluxes between the surface and atmosphere. Section 6 introduces the model parameters and numerical implementation. Section 7 describes the results obtained from the off-line experiments for different observational time series. CRREL, ARME and HAPEX-MOBULHY data are used to assess the scheme performance. Conclusions are presented in Section 8.

II. CONSERVATION EQUATIONS FOR WATER AND HEAT BALANCES

In IAP94, the control-volume method (cf. Patanka, 1980) is used and the equations are formulated in conservation form over control volume. Here our focus is only on a one-dimensional vertical media that has no lateral gradients. For numerical computation, the canopy, snow and soil are subdivided into n+1 layers with variable thickness $\Delta z_j (j = 1,2,\cdots, n+1)$. Moreover, in order to conveniently deal with the accumulation or ablation of snow at

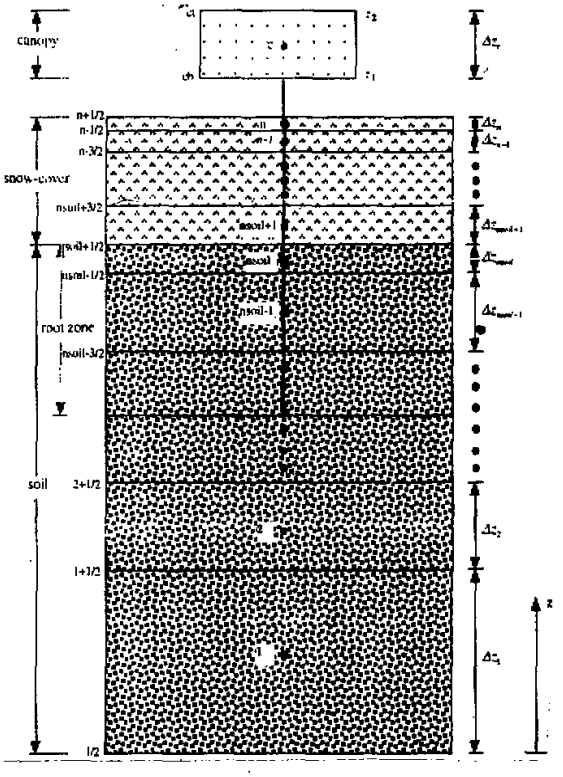

Fig. 1. Schematic diagram of the finite-difference grid structure of IAP94.

the top of the snow cover without renumbering the elements, an ascending order from the bottom up is indexed, as shown in Fig.1. Hereafter, superscripts j, $j+1/2$ and $j-1/2$, respectively, refer to the indices of control thickness Δz_j, and its upper and lower bounding surface.

In order to employ the mixture theory (Morland et al., 1990) and the dynamic theory of fluids in porous media (Bear, 1972), we first introduce a basic relation among the partial density γ_k, partial volume θ_k and intrinsic density ρ_k of constituent k, where the subscript k is i, l, v, a or d, respectively, for ice, liquid water, water vapor, air, or dry solids. They are related by

$$\gamma_k = \theta_k \rho_k, \tag{1}$$

where γ_k is defined as the mass of constituent k per unit volume of medium ($\mathrm{kgm^{-3}}$), ρ_k is the mass of constituent k per unit volume of constituent k ($\mathrm{kgm^{-3}}$), and θ_k is the volume fraction ($\mathrm{m^3m^{-3}}$) of constituent k. The mixture density ρ_t is given in terms of the partial densities by

$$\rho_t = \sum_k \theta_k \rho_k = \sum_k \gamma_k. \tag{2}$$

An alternative quantity, volume fraction of liquid-water at saturation, which also termed the voids "solid" porosity, will be used to refer to effective volume that liquid-water may occupy between the solids (ice plus solid) and written as

$$\theta_{l,sat} = 1 - \theta_i - \theta_d. \tag{3}$$

2.1 *Water Balance Equations*

Within a finite control thickness Δz_j of a medium, the time rate of change in mass must equal their net flow across the bounding surface, plus its rate of internal production. Since the matrices of soil and canopy are the immobile and incompressible invariant on the time scale of one month or less, additionally, the mass of dry air is negligible in comparison with other constituents (except water vapor), in essence, the mass balances are the water balances. The conservation equations for water phase k within control thickness Δz_j are written as follows,

$$\frac{\partial}{\partial t}\overline{\gamma_k \Delta z}^j = -[(U_k)^{j+1/2} - (U_k)^{j-1/2}] + \sum_{k'} \overline{M_{k'k}(1-\delta_{k'k})\Delta z}^j + \overline{S_k \Delta z}^j, \tag{4}$$

where $k', k = i,l,v,\delta_{k'k}$ = Kronecker delta, $M_{k'k}$ = rate of water phase k' to phase $K(\mathrm{kgm^{-3}s^{-1}})$, and $M_{k'k} = -M_{kk'}$, $U_k^{j+1/2}$, $U_k^{j-1/2}$, = mass flow of constituent k through the upper and lower bounding surface of control thickness $\Delta z_j(\mathrm{kgm^{-2}s^{-1}})$, respectively. Hereafter we prescribe the mass flow positive in the upward direction, S_k = internal source to contribute to constituent k.

Note that the sublimation is a very slow process by hand-to-hand within snowpack and soil media, here, except for top ground layer, we set $M_{iv} = 0$ for other ground layers. The movement of ice is negligible in comparison with the liquid water and water vapor, but except the accumulation of snowfall at the surface layer and in canopy. The internal sources S_k, here, are only for the transpiration from leaf stomatal and the plant abstraction from the root zone of soil layers.

Since each increase in one phase of water is balanced by a decrease in another, namely, $\sum_k \sum_{k'} \overline{M_{k'k}(1-\delta_{k'k})\Delta z}^j = 0$, hence by summing (4) for all water constituents, the conservation

for mixture water is expressed as

$$\frac{\partial}{\partial t}\overline{\rho_l \Delta z}^{j} = -\sum_k [(U_k)^{j+1/2} - (U_k)^{j-1/2}] + \sum_k \overline{S_k \Delta z}^{j}. \tag{5}$$

In (4) and (5), the overbar indicates a spatial integration over Δz_j, for a physical quantity Ω, the expression is

$$\overline{\Omega \Delta z}^{j} = \int_{z_{j-1/2}}^{z_{j+1/2}} \Omega dz. \tag{6}$$

Now let we transform the above constituents and mixture water balance equations into the familiar style used in previous LSPs. If we assume that the time change of water vapor within canopy is negligible, for water vapor equation (4) can be written as

$$\frac{\partial}{\partial t}\overline{\gamma_v \Delta z}^{c} = -(E_{ac} - E_{gc}) + E_w + E_{tr} \simeq 0, \tag{7}$$

where superscript "c" refers to the average over canopy; E_{ac}, E_{gc}, E_w and E_{tr} are the moisture fluxes ($\mathrm{kgm^{-2}s^{-1}}$), respectively, from canopy to atmosphere, ground to canopy space, wet foliage to canopy space, and transpiration.

By substituting (7) into (5), we can obtain balance equation for the mixture of liquid water and ice on foliage as

$$\frac{\partial W_{dew}}{\partial t} = \frac{1}{\rho_l}[-(U_v^{ct} - U_v^{cb}) - E_w], \tag{8}$$

where superscripts "*ct*" and "*cb*" are the index of top and bottom of canopy, subscript ϑ refers to i or l (for snowfall $\vartheta = i$, for rainfall $\vartheta = l$), W_{dew} is equivalent-water depth (a transformation of water mass) stored on foliage (m).

By (1), we can write (4) for liquid water within snow or soil media in terms of water volumetric content as follows:

$$\frac{\partial \overline{\theta_l}^{j}}{\partial t} = \frac{1}{\rho_l \Delta z_j}[-(U_l^{j+1/2} - U_l^{j-1/2}) + \overline{M_{il} \Delta z}^{j} - \overline{M_{lv} \Delta z}^{j}$$
$$- \delta E_{tr}^{j}] - (1-\delta)\overline{\theta_l}^{j}\frac{1}{\Delta z_j}\frac{\partial \Delta z_j}{\partial t}. \tag{9}$$

The last term on right hand side in (9) represents the loss of liquid water due to the compaction of snow, in which δ is the delta function ($\delta = 1$ for soil, $\delta = 0$ for snowpack). E_{tr}^{j} is the rate of plant abstraction of liquid water from jth soil layer ($\mathrm{kgm^{-2}s^{-1}}$). For surface layer, $\overline{M_{lv} \Delta z}^{1} = E_{gb} + E_{gc}$.

2.2 *Heat Balance Equations*

Analogous to the conservation equations for water, the conservation of heat stipulates that the time rate of change in stored heat within thickness Δz_j equals the net heat flux across the upper and lower bounding surface plus the internal heat sources. Provided that the forcing time scale is much longer than the time scale for thermal transfer among the component ice, liquid-water and dry solid, we may assume that they are in a state of thermal equilibrium, namely, assume that they have a common temperature T. Moreover, the air (water and dry air) mass is of a lower order in comparison with other components in media, their heat capacity may be negligible. If we further assume the control variables T to be stepwise-homogeneous within control thickness Δz_j, then the heat conservation equation for the mixture of

solid matrix, ice and liquid water, and for the air component can be written as

$$\begin{aligned}&\sum_{k=i,l,d}\overline{\gamma_k c_k \Delta z}^{j}\frac{\partial T_j}{\partial t}+\sum_{k=i,l}[(c_k TU_k)^{j+1/2}-(c_k TU_k)^{j-1/2}-c_k T_j(U_k^{j+1/2}-U_k^{j-1/2})]\\&=\left[\left(\lambda'_e\frac{\partial T}{\partial z}\right)^{j+1/2}-\left(\lambda'_e\frac{\partial T}{\partial z}\right)^{j-1/2}\right]+\overline{h(T_a-T)\Delta z}^{j}+[I_R^{j+1/2}-I_R^{j-1/2}]\\&-\sum_{k}\sum_{k'\neq k}\overline{L_{k'k}M_{k'k}(1-\delta)\Delta z}^{j}-\delta L_{lv}E'_{tr}\end{aligned}\qquad(10)$$

and

$$\left(\lambda'_a\frac{\partial T_a}{\partial z}\right)^{j+1/2}-\left(\lambda'_a\frac{\partial T_a}{\partial z}\right)^{j-1/2}+\overline{h(T-T_a)\Delta z}^{j}\approx 0,\qquad(11)$$

where

T_j= averaged common temperature of the mixture of ice, liquid water and dry solid over $\Delta z_j(K)$,

T_a= averaged air temperature over $\Delta z_j(K)$,

c_k= specific heat of component k ($\mathrm{Jkg^{-1}K^{-1}}$),

$L_{k'k}$= latent heat due to the water phase change, and $L_{k'k}=-L_{kk'}$, $(k=i,l,v)$ ($\mathrm{Jkg^{-1}}$),

I_R= radiation flux (solar radiation and atmospheric longwave radiation) ($\mathrm{Wm^{-2}}$), positive in downward direction,

λ'_e= effective thermal conductivity of mixture of ice, liquid water and dry solid ($\mathrm{Wm^{-1}K^{-1}}$), and, $\lambda'_e=\sum_{k=i,l,d}\theta_k\lambda_k$, in which λ_k is the thermal conductivity of component k $(k=i,l,d)$,

h= coefficient of heat transfer between air and mixture of ice, liquid water and dry solid ($\mathrm{Wm^{-2}K^{-1}}$),

δ = delta function, here, $\delta=1$ for canopy, $\delta=0$ for snowpack or soil.

The second term on left hand side in (10) represents the heat loss through the water flow. The second term on right hand side in (10) is the heat transfer flux between air and the bounding surface of mixture of ice, liquid-water and dry solid. Here we assume that this heat transfer only occurs in canopy, namely, all constituents maintain a common temperature for snowpack and soil within a control thickness. The fourth term on the right hand side in (10) is the latent heat due to the phase change in Δz_j. Here we assume that the gains and loss of latent heat are constrained to mixture of ice, liquid-water and dry solid. Eq. (11) holds only for air in canopy.

With the common assumption made in current LSPs that the bulk thermal conductivity of the mixture of water (liquid and solid water) on foliage, and the heat capacity of canopy space are negligible, (10) and (11) are reduced to

$$\begin{aligned}&\overline{\rho_l c_l \Delta z}^{c}\frac{\partial T_c}{\partial t}+\sum_{k=i,l}[(c_k TU_k)^{ct}-(c_k TU_k)^{cb}-c_k T_c(U_k^{ct}-U_k^{cb})]\\&=-[H_c+L_{\sigma l}E_w+L_{lv}E_{tr}]-\overline{L_{il}M_{il}\Delta z}^{c}+[I_R^{ct}-I_R^{cb}]\end{aligned}\qquad(12)$$

and

$$-H_{ac}+H_{gc}+H_c\simeq 0,\qquad(13)$$

where

$\vartheta = i$ or l (for sublimation $\vartheta = i$, for evaporation $\vartheta = l$), T_c = averaged foliage temperature over canopy (K), H_c = sensible heat flux between foliage and canopy space air (Wm^{-2}), H_{gc} = sensible heat flux between ground and canopy (Wm^{-2}), H_{ac} = sensible heat flux between canopy and reference height (Wm^{-2}), $\overline{\rho_l c_l \Delta z}^c$ = bulk heat capacity of canopy, in present model, we assume that it is of the order of the heat capacity of 0.2 mm of water per unit leaf area index, namely,

$$\overline{\rho_l c_l \Delta z}^c = [0.0002 LAI \times F_{veg}(1 - F_{sn}) + W_{dew}] \times 4.295 \times 10^6 (Jm^{-1}K^{-1}), \tag{14}$$

where LAI is the total leaf area index, F_{veg} the canopy cover fraction, and F_{sn} the fraction of vegetation covered by snow.

Provided that the forcing time scale is much longer than the time scale for thermal transfers among constituents to take place in control thickness Δz_j for soil and snow media, we can assume that all the constituents are in a state of thermal equilibrium, i.e., all constituents have a common temperature T. Moreover, the sublimation of solid water within media is absent in our model, but it only occurs at the surface of top layer. Thus, there is a single mixture energy equation for soil or snow media. By summing (10) and (11), the heat balance equations for the internal and top control thickness of ground can be written as

$$\begin{aligned}&\overline{\rho_l c_l \Delta z}^j \frac{\partial T_j}{\partial t} + [(c_l T U_l)^{j+1/2} - (c_l T U_l)^{j-1/2} - c_l T_j (U_l^{j+1/2} - U_l^{j-1/2})] \\ &= \left[\left(\lambda_e \frac{\partial T}{\partial z}\right)^{j-1/2} - \left(\lambda_e \frac{\partial T}{\partial z}\right)^{j-1/2}\right] - [\overline{L_{il} M_{il} \Delta z}^j + \overline{L_{lv} M_{lv} \Delta z}^j] + [I_R^{j+1/2} - I_R^{j-1/2}]\end{aligned} \tag{15}$$

and

$$\begin{aligned}&\overline{\rho_l c_l \Delta z}^n \frac{\partial T_n}{\partial t} + \sum_{k=i,l} [(c_k T U_k)^{n+1/2} - (c_k T U_k)^{n-1/2} - c_k T_j (U_k^{n+1/2} - U_k^{n-1/2})] \\ &= -[(H_{gb} + L_{\theta_l} E_{gb}) + (H_{gc} + L_{\theta_l} E_{gc})] - \left(\lambda_e \frac{\partial T}{\partial z}\right)^{n-1/2} - \overline{L_{il} M_{il} \Delta z}^n + [I_R^{n+1/2} - I_R^{n-1/2}]\end{aligned} \tag{16}$$

where the superscript "n" refers to the top ground control thickness; H_{gb}, H_{gc} are sensible heat (Wm^{-2}) from soil or snow surface to atmosphere, respectively, for the fraction of non-vegetated and vegetated ground; E_{gb}, E_{gc} are the rate of evaporation or sublimation ($kgm^{-2}s^{-1}$), respectively, for the fraction of non-vegetated ground and vegetated ground, and positive in upward direction. The bulk heat capacity $\overline{\rho_l c_l \Delta z}^j$ is expressed by

$$\overline{\rho_l c_l \Delta z}^j = \begin{cases} \sum_{k=i,l} \overline{\gamma_k c_k \Delta z}^j & \text{for snow} \\ \sum_{k=i,l,d} \overline{\gamma_k c_k \Delta z}^j & \text{for soil} \end{cases} \tag{17}$$

The effective thermal conductivity of soil is computed from the algorithm of Johansen (as recommended by Farouki, 1981), and that of snow is from SNTHERM.89 (Jordan, 1991), which are expressed by

$$\lambda_e = (\lambda_{sat} - \lambda_{dry})\lambda_c + \lambda_{dry} \tag{18a}$$

for soil, and

$$\lambda_e = 0.023 + (7.75\gamma_w + 0.1105\gamma_w^2) \times 10^{-5} \times 2.267(Wm^{-1}K^{-1}) \quad (18b)$$
$$(\gamma_w = \gamma_i + \gamma_l)$$

for snow. In (18a), λ_{sat} and λ_{dry} are the thermal conductivity of saturated and dry soil respectively, λ_c is a normalized thermal conductivity, i.e. a function of porosity fractional saturation and soil quartz content (Farouki, 1981, p.112).

Once the conservation laws are written down, a model must formulate the various parameterization relationships describing the fluxes and the constituent properties and the interactions. The parameterization of the fluxes of energy and water flow that are employed by equations in this section will be presented in following three sections.

III. WATER FLUXES WITHIN SOIL, SNOW AND CANOPY

3.1 *Water Fow in Canopy*

Precipitation arriving at the vegetation top either is intercepted by foliage, or falls through gaps of the leaves in the canopy to the ground. Following Sellers et al. (1996), the rate of inflow (interception), the rate of outflow (drainage of water stored on the vegetation), and the rate of precipitation through foliage are given by

$$U_{\vartheta}^{cf} = -\rho_l F_{veg} P_0 [1 - \exp(-K_e LAI / F_{veg})], \quad (19)$$

$$U_{\vartheta}^{cb} = -\rho_l D_c, \quad (20)$$

where P_0 is the rate of atmospheric precipitation (ms^{-1}); D_c the rate of canopy drainage (ms^{-1}) (here the formulation (D7) of Sellers et al. (1996) are used); K_e the extinction coefficient for rainfall, as same as for vertical direct beam of radiation described in SiB; and the subscript refers to i or l (for snowfall $\vartheta = i$, for rainfall $\vartheta = l$). The precipitation, P_g, reaching the ground surface, can be divided into two parts: one is what directly arriving at the top of the bare ground and through the gaps in canopy to the ground P'_g, and the other is the canopy drainage P''_g:

$$P''_g = \rho_l D_c, \quad (21)$$

$$P'_g = \rho_l P_0 [(1 - F_{veg}) + F_{veg} \exp(-K_e LAI / F_{veg})], \quad (22)$$

$$P_g = P'_g + P''_g. \quad (23)$$

3.2 *Surface Runoff and Infiltration*

Rainfall incident on ground either infiltrates the soil (or snow, if snow cover exists), or becomes surface runoff when its rate is greater than the maximum infiltration of ground surface layer or the surface layer is saturated. For snowfall it will be accumulated at the surface. The surface runoff and infiltration fluxes (the water generated by the melted snow will be considered as an internal process, hence is not included here) are expressed as

$$Y(0) = 0, \quad (24a)$$

$$\left.\begin{aligned} U_l^{n+1/2} &= -P_g \\ U_l^{n+1/2} &= 0 \end{aligned}\right| \quad (25a)$$

for snowfall, and

$$Y(0)=\frac{1}{\rho_l}\times\begin{cases}P_g-\mathrm{Min}(P_g,\rho_l K_{sat}), & \text{when } \overline{\theta_l}^n<\overline{\theta_{l,sat}}^n\\ P_g & \text{when } \overline{\theta_l}^n\geq\overline{\theta_{l,sat}}^n\end{cases} \tag{24b}$$

$$\left.\begin{aligned}U_l^{n+1/2}&=0\\ U_l^{n+1/2}&=-[P_g-Y(0)\rho_l]\end{aligned}\right| \tag{25b}$$

for rainfall, where $Y(0)$ is the rate of surface runoff (ms^{-1}), and K_{sat} the hydraulic conductivity of saturated soil or snow (ms^{-1}).

3.3 *Water Flow in Soil*

The Darcy law is used for calculating the water flow in soil

$$U_l=-\rho_l K\frac{\partial}{\partial z}(\psi+z), \tag{26}$$

where K is the hydraulic conductivity (ms^{-1}), and ψ the water potential (m), which are related to θ_l through a set of simple relationships found in Clapp and Hornberger (1978)

$$K(\theta_l)=K_{sat}(\theta_l/\theta_{l,sat})^{2B+3}, \tag{27}$$

$$\psi(\theta_l)=\psi_{sat}(\theta_l/\theta_{l,sat})^{-B}, \tag{28}$$

where K_{sat} is the saturated hydraulic conductivity (ms^{-1}),ψ_{sat} the saturated water potential (m), and B the slope of the retention curve of soil water. The expression of finite difference of (24) is described in Appendix B.

At the bottom of soil layer, there is gravitational drainage that dominates the flow for large-enough length scales. According to the presumption of gravitational flow, the water flow at the soil bottom $U_l^{1/2}$ can be given by

$$U_l^{1/2}=-\rho_l K_b(\theta_l/\theta_{l,sat})^{2B+3}, \tag{29}$$

where K_b is the saturated hydraulic conductivity at the bottom (ms^{-1}).

3.4 *Water Flow in Snow*

Since the capillary forces with snow are usually two to three orders of magnitude less than those of gravity (Colbeck, 1971), based on Jordan (1991) simplification, we can write the water flux as

$$U_l=-\frac{K_l}{\mu_l}\rho_l^2 g, \tag{30}$$

where g is the gravitational acceleration (ms^{-2}), μ_l dynamic viscosity (here assuming that it has a value of 1.787×10^{-3} Nsm^{-1} at 0°C), and K_l the hydraulic permeability (m^{-2}),

$$K_l=K_{\max}s_e^3, \tag{31}$$

$$K_{\max}=0.077d^2\exp(-0.0078\gamma_i), \tag{32}$$

where $K_{\max}$ is the saturation permeability, s_e the effective liquid saturation defined by $s_e=\dfrac{\theta_l-\theta_{l,r}}{\theta_{l,sat}-\theta_{l,r}}$, $\theta_{l,r}$ the irreducible liquid-water volumetric content in snowpack ($0.014\theta_{l,sat}-0.069\theta_{l,sat}$), and d the mean grain diameter (m). The expression of finite difference of (30) is

described in Appendix B.

3.5 *Vapor Diffusion in Soil*

Vapor movement should be taken into account only in the soil media in which soil temperature is great than 273.15K and water content less than 3% (Mehta et al., 1994). The movement of water vapor in soil takes two forms: one is the molecule diffusion, and the other is the convection conducted by pumping at the surface. In present step, we only consider the former. The flux of molecule diffusion can be described by Fick law

$$U_v = -D_v \frac{d\rho_v}{dz}, \tag{33a}$$

where D_v is the effective coefficient of diffusion (m^2s^{-1}). For this term, we currently use the empirical express combined from Milly (1984) and Kimball (1976),

$$D_v = 229 \times 10^{-7} \left(\frac{T}{273.15}\right)^{1.75} \left(\frac{1000}{P_s}\right)(\theta_{l,sat} - \theta_l)^{5/3}, \tag{34}$$

where T is the temperature of media (K), and P_s the surface atmospheric pressure (hPa). In (33a), ρ_v is the water vapor density in the media (kgm^{-3}), which is usually expressed as following Philip's formulation (1957)

$$\rho_v = h_r \rho_{sat}, \tag{35}$$

$$h_r = \exp\left(\frac{\psi g}{R_w T}\right), \tag{36}$$

$$\rho_{sat} = \frac{e_{sat}(T)}{R_w T}. \tag{37}$$

Although Philip's formulation is applicable only if an equilibrium between liquid-water and the vapor in soil pores is maintained, and is invalid near the surface of a natural soil, it is still a good choice now, since there is only one investigation on loam that made by Kondo et al. (1990, 1992). It follows from (33a) and (34)-(37) that

$$U_v \approx -D_v C_\theta \frac{\partial \theta_l}{\partial z}, \tag{33b}$$

$$C_\theta = \frac{h_r g}{(R_w T)^2} \frac{B\psi_{sat}}{\theta_{l,sat}} \left(\frac{\theta_l}{\theta_{l,sat}}\right)^{-B-1},$$

where R_w is the gas constant of vapor ($Jkg^{-1}K^{-1}$), g the gravitational acceleration (ms^{-2}), and $e_{sat}(T)$ the saturated vapor pressure at temperature T. Note that the dependence of vapor diffusion on the temperature gradient is neglected in (33b) for simplicity, since it is lower order of magnitude compared to the effect of capillary. The expression of finite difference of (33) is described in Appendix B.

3.6 *Snow Compaction and Grain Size*

Snow compaction is caused by its metamorphisms. According to Yen (1980), there are four types, namely, destructive metamorphism, pressure metamorphism, constructive metamorphism, and melt metamorphism. In present study, the former two metamorphisms are considered for simplicity. The scheme is from Jordan (1991) which is sorted out from Anderson (1976),

$$CR = -\frac{1}{\Delta z}\frac{\partial \Delta z}{\partial t} = -\left|\frac{1}{\Delta z}\frac{\partial \Delta z}{\partial t}\right|_{metamorphism} - \left|\frac{1}{\Delta z}\frac{\partial \Delta z}{\partial t}\right|_{overburden} \tag{38}$$

The mean grain diameter, $d(m)$, is a critical variable in both mass and energy balance equations, in that it affects (among other things) the permeability of snow to fluid flow, surface albedo and extinction coefficient for solar radiation. The formulation is taken from Anderson (1976)

$$d = \begin{cases} 0, & \text{if } \gamma_i \geqslant 917 \quad \text{kgm}^{-3} \\ 2.976 \times 10^{-3}, & \text{if } 400 \leqslant \gamma_i \leqslant 917 \quad \text{kgm}^{-3} \\ 1.6 \times 10^{-4} + 1.1 \times 10^{-13}\gamma_i^2, & \text{if } \gamma_i < 400 \quad \text{kgm}^{-3} \end{cases} \tag{39}$$

IV. RADIATION FLUXES

In this section, we first present the parameterization of the fraction of ground cover, which is useful in calculating the grid averaged values of the surface fluxes, and then, briefly describe how to calculate the surface albedo and radiative fluxes.

4.1 *Fraction of Ground Cover*

Our model permits limited heterogeneity at the land surface such that bare soil, vegetation and snow cover can coexist simultaneously in a grid square. First of all we assume that the fraction of bare ground and vegetation cover is time-invariant in a time step, therefore, what needed to be predicted is the variation of the fractions of snow cover with the accumulation or ablation of snow. Following the formulations of BATS (Dickinson et al., 1986; 1993), the fraction of soil and vegetation covered by snow is expressed as

$$S_{cv} = \text{snowdepth} / (0.1 + \text{snowdepth}), \tag{40}$$

$$F_{sn} = \text{snowdepth} / (10 z_{CM} + \text{snowdepth}), \tag{41}$$

where S_{cv} is the fraction of ground covered by snow, F_{sn} is the fraction of vegetation covered by snow, *snowdepth* is the snow depth covered on ground (m), and z_{CM} is the aerodynamic roughness of vegetation (m). Furthermore, each grid square over land may conceptually be divided into four fractions,

$F_V = F_{veg}(1 - F_{sn})$, vegetation fraction without snow covered,
$F_B = (1 - F_{veg})(1 - S_{cv})$, ground fraction without snow covered,
$F_{VS} = F_{veg} F_{sn}$, vegetation fraction with snow covered,
$F_{BS} = (1 - F_{veg}) S_{cv}$, ground fraction with snow covered.

4.2 *Surface Albedo*

The solar spectrum in our model is partitioned into two wavebands (visible and near-infrared with the boundary at 0.7 μm) for both the diffuse and direct beam contributions. Surface albedo calculations are performed for these four components using mean spectral properties for each wavelength interval. The albedo schemes of BATS (for soil and snow) and SiB (for canopy) are adopted, but two aspects of modification have been done in our model. They are:

(1) The ground albedo $\alpha_{g,\Lambda,\chi}$ is calculated as a function of snow-free albedo $\alpha_{b,\Lambda,\chi}$, deep snow albedo $\alpha_{s,\Lambda,\chi}$, and snow equivalent -water depth d_{sw}(m), given by

$$\alpha_{g,\Lambda,\chi} = \begin{cases} \alpha_{b,\Lambda,\chi} + d_{sw}^{1/2}(\alpha_{s,\Lambda,\chi} - \alpha_{b,\Lambda,\chi}) & \text{when} \quad d_{sw} < d_{swmax} \\ \alpha_{s,\Lambda,\chi} & when \quad d_{sw} \geqslant d_{swmax} \end{cases}, \tag{42}$$

where subscripts "g", "b" and "s" refer to ground, bare soil and snow cover respectively, Λ refers to the solar wavebands (visible and near-infrared), χ refers to the incident direction of radiation (direct and diffuse), and d_{swmax} is the critical depth where the effect of ground on snow surface albedo may be neglected, which is generally taken as 0.01 (m).

(2) Based on above ground albedo, we recalculate the canopy radiative transfer equations (two-stream approximation equation) (Sellers, 1985) for one vegetation layer.

The grid mean albedo $\bar{\alpha}_{\Lambda,\chi}$ is given by a simple area weighted average as follows:

$$\bar{\alpha}_{\Lambda,\chi} = (1 - F_V)\alpha_{g,\Lambda,\chi} + F_V \alpha_{c,\Lambda,\chi}, \tag{43}$$

where $\alpha_{c,\Lambda,\chi}$ is the albedo of canopy.

4.3 *Net Radiation Fluxes Absorbed by Surface*

The solar radiation absorbed by canopy and that by ground are given by

$$F_{c,\Lambda,\chi} = F_V[(1 - \alpha_{c,\Lambda,\chi}) - \tau_{\Lambda,\chi}(1 - \alpha_{g,\Lambda,dif}) - \tau_{3,\Lambda}(1 - \alpha_{g,\Lambda,\chi})]Rads_{\Lambda,\chi}, \tag{44}$$

$$F_{g,\Lambda,\chi} = \{(1 - F_V)(1 - \alpha_{g,\Lambda,\chi}) + F_V[\tau_{\Lambda,\chi}(1 - \alpha_{g,\Lambda,dif}) + \tau_{3,\Lambda}(1 - \alpha_{g,\Lambda,\chi})]\}Rads_{\Lambda,\chi}, \tag{45}$$

respectively, where

$Rads_{\Lambda,\chi}$ = incident solar radiation of wavelength interval Λ and direction χ (*dir*= direct, *dif*= diffuse) (Wm^{-2}),

$F_{c,\Lambda,\chi}$ = solar radiation absorbed by canopy (Wm^{-2}),

$F_{g,\Lambda,\chi}$ = solar radiation absorbed by ground (Wm^{-2}),

$\tau_{\Lambda,\chi}$ = diffuse fluxes per unit incident direct beam and diffuse radiation leaving base of canopy (downward),

$\tau_{3,\Lambda}$ = direct beam flux transmitted through the canopy per unit incident, for diffuse flux calculation, $\tau_{3,\Lambda} = 0$.

By summing the net longwave radiation fluxes, the total radiation absorbed by canopy and ground is given by

$$I_R^{ct} - I_R^{cb} = \sum_{\Lambda}\sum_{\chi} F_{c,\Lambda,\chi} + F_V \delta_t [Radl + \varepsilon_s \sigma (T_n)^4 - 2\varepsilon_c \sigma (T_c)^4], \tag{46}$$

$$I_R^{n+1/2} = \sum_{\Lambda}\sum_{\chi} F_{g,\Lambda,\chi} + (1 - F_V \delta_t)Radl + F_V \delta_t \varepsilon_c \sigma (T_c)^4 - \varepsilon_s \sigma (T_n)^4, \tag{47}$$

where *Radl* is the downward atmospheric longwave radiation (Wm^{-2}); ε_s and ε_c are ground and canopy emissivity, respectively, the value range is 0.9 – 1.0 (Kondrayev et al., 1981); σ Stefan-Boltzmann constant ($Wm^{-2}K^{-4}$); δ_t the canopy transmittance for thermal radiation, and

$$\delta_t = 1 - \exp\{-\max[10^{-5}, \min(50, LAI / (F_{veg}\bar{\mu}))]\}, \tag{48}$$

where $\bar{\mu}$ is the averaged inverse diffuse optical depth per unit leaf area. Note that the detailed formulations of the coefficients of radiation reflectance and transmission in (44) – (46) have been presented by Sellers et al. (1985, 1986).

Snow is not opaque to solar radiation, in the presence of snow on ground, the radiation transmission should be taken into account. According to Jordan's assumption (1991) that the extinction of infrared radiation is constrained to a thickness of 2 mm of surface snow layer,

we may assume that all incident infrared radiation will be absorbed in surface layer since the thickness of surface layer prescribed in our model is far larger than 2mm. Therefore, what we should consider is only the transmission of visible radiation in snow. The extinction coefficient is given by

$$\beta_{vis} = \frac{0.003795\gamma_w}{\sqrt{d}}. \tag{49}$$

The energy gain due to radiation heating within snow cover can be expressed by

$$I_R^{n+1/2} - I_R^{n-1/2} = I_R^{n+1/2} - \sum_{\chi=dir,dif} F_{g,vis,\chi} \exp(-\beta_{vis}\Delta z_n) \tag{50}$$

for surface snow layer and

$$I_R^{j+1/2} - I_R^{j-1/2} = I_R^{j+1/2}[1 - \exp(-\beta_{vis}\Delta z_j)] \tag{51}$$

for interior snow layer *j*. The radiation transmitted out of the bottom of the snowpack will be absorbed by the underlying surface soil layer *nsoil*.

V. FLUXES OF SENSIBLE HEAT AND EVAPOTRANSPIRATION

In our model the surface fluxes of sensible heat and evapotranspiration are calculated by means of the classical resistance formulation in the electrical analog form

$$\text{flux} = \frac{\text{potential difference}}{\text{resistance}}.$$

The potential differences are represented by temperatures, specific humidities, respectively. The resistances are equivalent to the integrals of inverse conductance over a path between the specified potential difference endpoints. Fig.2 shows how the fluxes of sensible heat,

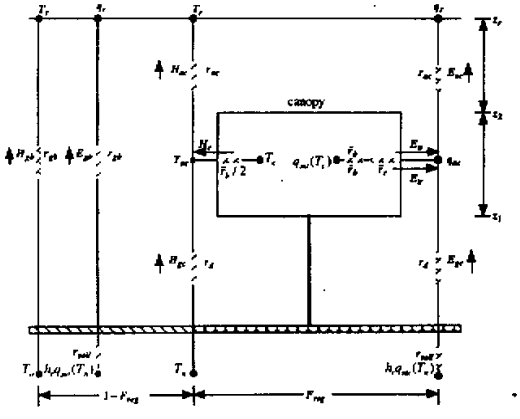

Fig.2. Schematic description of transfer pathway for sensible heat and moisture / latent heat between land-surface and reference height.

evaporation and transpiration from ground and canopy traverse the aerodynamic resistances (r_{ac}, r_{ag}, r_d, $\bar{r}_b$), and surface resistances (r_{soil}, $\bar{r}_c$). Fluxes, potential differences, and resistances in Fig.2 are summarized in Table 1.

Table 1. Fluxes, Fraction of Cover, Potential Differences, and Resistances

Flux	Fraction of cover	Potential difference	Resistance
H_{gb}	$1-F_V$	$\rho_{air}c_p(T_n-T_r)$	r_{ag}
H_{gc}	F_V	$\rho_{air}c_p(T_n-T_{ac})$	r_d
H_c	F_V	$\rho_{air}c_p(T_c-T_{ac})$	$\bar{r}_b/2$
H_{ac}	F_V	$\rho_{air}c_p(T_{ac}-T_r)$	r_{ac}
E_{gb}	$1-F_V$	$\rho_{air}[h_r q_{sat}(T_n)-q_r]$	$r_{ag}+r_{soil}$
E_{gc}	F_V	$\rho_{air}[h_r q_{sat}(T_n)-q_{ac}]$	r_d+r_{soil}
E_w	$F_V\delta$	$\rho_{air}[q_{sat}(T_c)-q_{ac}]$	$\bar{r}_b$
E_{tr}	$F_V(1-\delta)$	$\rho_{air}[q_{sat}(T_c)-q_{ac}]$	$\bar{r}_b+\bar{r}_c$
E_{ac}	F_V	$\rho_{air}[q_{ac}-q_r]$	r_{ac}
T_r, q_r = air temperature and specific humidity at the reference height (K, kgkg^{-1})			
T_{ac}, q_{ac} = air temperature and specific humidity in canopy space (K, kgkg^{-1})			
ρ_{air}, c_p = air density and specific heat (kgm^{-3}, Jkg^{-1}K)			
r_{ag} = aerodynamic resistance between bare ground and reference height (sm^{-1})			
r_d = aerodynamic resistance between ground and canopy air space (sm^{-1})			
r_{ac} = aerodynamic resistance between canopy air space and reference height (sm^{-1})			
$\bar{r}_b$ = bulk canopy boundary layer resistance (sm^{-1})			
$\bar{r}_c$ = bulk canopy stomatal resistance (sm^{-1})			
r_{soil} = soil surface resistance (sm^{-1})			
h_r = relative humidity within pore space of surface soil layer			
$q_{sat}(T)$ = saturated specific humidity at temperature T (kgkg^{-1})			
δ = wetted fraction of canopy, as in BATS, $\delta = (W_{dew}/W_{dewmax})^{2/3}$			

In the following subsections, each resistance in the surface flux formulations in Table 1 will be briefly described with canopy parameters (canopy height, leaf area index, leaf drag coefficient, etc.), external conditions (meteorological conditions at reference height), and unknown variables (such as temperature T_c, T_n and moisture content $\overline{\theta_l}^*$). The surface roughness length and zero-plane displacement height are two important surface characteristic limits that largely influence the magnitude of aerodynamic resistances and near-surface turbulent transfer. For this reason, at first, we will pay a great attention to them.

5.1 *Surface Roughness Length and Zero-Plane Displacement Height of Canopy*

In the case of rough surfaces, the effective source height for sensible and latent heat transfers is not the same as that for momentum. Many researchers have stressed that in surface layer parameterization, the roughness length value for heat (moisture) must be different from that from momentum (Brutsaert, 1979; Garratt, 1992, 1993; etc.). Recently, Chen et al.(1996) have tested the influence of the heat (moisture) roughness length in three atmospheric surface layer parameterization schemes (Mellor-Yamada, Paulson, and modified Louis), and found that they are more sensitive to the treatment of roughness length for heat (moisture), rather than the choice among the three surface layer schemes. Following the relations summarized by Verseghy et al. (1993), the relations used to obtain z_H from z_M for the

four major ground cover types can be rewritten as follows:

$z_{CH}=z_{CM}/2$ for forest
$z_{CH}=z_{CM}/7$ for crop
$z_{CH}=z_{CM}/12$ for grass
$z_{GH}=z_{GM}/3$ for bare soil and snow cover

where z_{GH} and z_{GM} are the heat (moisture) roughness and aerodynamic roughness for ground, respectively. Here, we assume $z_{GM}=10^{-2}$ (m) for bare soil, and $z_{GM}=10^{-3}$ (m) for snow cover; z_{CH} and z_{CM} are the heat (moisture) roughness and aerodynamic roughness for canopy, respectively. For the case of vegetation cover, the aerodynamic roughness is related to the density and height of canopy, and the underlying ground roughness length. Following Yamazaki et al. (1992) formulations, it is given by

$$z_{CM}=z_2\left(1-\frac{d}{z_2}\right)\exp\left\langle-\left\{\left(1-\frac{d}{z_2}\right)\times\left[f\frac{c_{*1}}{2k^2}+\frac{1-f}{\ln(z_2/z_{GM})}\right]\right\}^{-1}\right\rangle, \tag{52}$$

where d is the zero-plane displacement of canopy, and

$$d=z_2\left\{1-\left(\frac{z_1}{z_2}-\frac{2k^2}{c_*}\right)\times\exp\left[-\frac{c_*}{2k^2}\left(1-\frac{z_1}{z_2}\right)\right]-\frac{2k^2}{c_*}\right\}. \tag{53}$$

In (52) and (53), z_2 and z_1 are the height of top and bottom of canopy respectively, k the von Karman constant, and c_* the nondimensional canopy density,

$$c_*=c_d LAI, \tag{54}$$

where c_d is the drag coefficient of individual leaves. f is a weighting function,

$$f=\frac{0.494(x+0.8)}{[(x+0.8)(x-0.5)+1.1]^{1/2}}+0.37, \quad (-3\leqslant x\leqslant 1) \tag{55}$$

$$x=\ln c_*$$

$$\ln c_{*1}=\frac{(x+0.26)+[(x+0.26)^2+0.16]^{1/2}}{2}, \quad (-3\leqslant x\leqslant 1) \tag{56}$$

where c_{*1} is a modified canopy density.

5.2 *Wind Profile above and within Canopy*

In AGCM or uncoupled LSP simulations, the surface wind speed they provided is only the wind speed u_r at a reference height. Therefore, it is necessary to obtain a wind profile from u_r. When the surface that is either bare or covered by fine roughness not exceeding several centimeters in height, the wind profile is usually described by the logarithmic law. To extend the logarithmic law to turbulent flow over relatively high roughness, such as tall vegetation or forest canopies, a purely empirical modification is advanced. At present studies, an extrapolation of log-linear wind profile is adopted for above canopy, which is from Xue et al.(1991), and written as follows:

$$u=u_r-\frac{u_*}{k}\left[\ln\frac{z-d}{z_{CM}}\right]_{z_1}^{z}-0.75\frac{u_*}{k}\left[\ln\frac{z-d}{z_{CM}}\right]_{z_2}^{z_1}, \tag{57}$$

where u is the wind speed above canopy, u_* the friction velocity, and z_1 the transition height,

$$z_1=z_2+11.785z_{CM}. \tag{58}$$

In dense canopy the wind coincides with the exponential profile (Inoue, 1963). To satisfy a wide vegetation covers existing in the global land, the wind speed within canopy is expressed by the sum of the logarithmic term and exponential term. An extrapolation of log-linear and exponential-line wind profile that is from Yamazaki et al. (1992) is adopted as follows:

$$u = u_2 \left\{ f \times \exp\left[-\frac{c_{*1}}{2k^2} \left(1 - \frac{z}{z_2} \right) \right] + (1 - f) \times \frac{\ln z / z_{GM}}{\ln z_2 / z_{GM}} \right\}. \tag{59}$$

Within the trunk space ($z < z_1$), the log-linear wind profile is assumed by

$$u = u_1 \frac{\ln z / z_{GM}}{\ln z_1 / z_{GM}}, \qquad (z_{GM} \leqslant z \leqslant z_1). \tag{60}$$

In above considerations, for simplicity, only the case of neutral stability atmospheric boundary layer is taken into account.

5.3 *Aerodynamic Resistances and Surface Resistances*

5.3.1 Aerodynamic resistances and friction velocity

The aerodynamic resistances and friction velocity can conventionally be obtained by solving the Businger-Dyer flux-gradient relationships (Dyer, 1974), however, a costly iterative process has to be used. In order to avoid iterations during model integration, Louis' empirical approach (Louis et al., 1982) is adopted in our model. This approach is based on a bulk Richardson number and provides explicit formulations for the calculations, however, it is shown that the result for the cases of unstable atmospheric stratification is better than that for the stable case. In order to overcome this shortcoming, the modified Louis approach introduced by Mahrt (1987) is adopted. Additionally, the different values of the roughness length for heat and momentum are implemented. The formulations of the aerodynamic resistances and friction velocity are written as follows:

$$r_{ag}^{-1} = \frac{k^2 u_r}{\ln(z_r / z_{GM}) \ln(z_r / z_{GH})} f_h(z_r / z_{GH}, RiB), \tag{61}$$

$$r_{ac}^{-1} = \frac{k^2 u_r}{\ln[(z_r - d) / z_{CM}] \ln[(z_r - d) / z_{CH}]} f_h[(z_r - d) / z_{CH}, RiB], \tag{62}$$

$$r_d^{-1} = \frac{k^2 u_r}{\ln(z_1 / z_{GM} + 1) \ln(z_1 / z_{GH} + 1)}, \tag{63}$$

$$u_*^2 = \left\{ \frac{k}{\ln[(z_r - d) / z_{CM}]} \right\}^2 u_r^2 f_m[(z_r - d) / z_{CM}, RiB], \tag{64}$$

where f_h and f_m are the Louis' empirical function (see Louis et al., 1982; Mahrt, 1987), RiB is the bulk Richardson number and defined as

$$RiB = \frac{gz\Delta T}{T_r u_r^2}, \tag{65}$$

where g is the gravity acceleration, $z = z_r - d$ for canopy, $z \approx z_r$ for ground, $\Delta T = T_r - T_{ac}$ for canopy, $\Delta T = T_r - T_n$ for ground.

5.3.2 Bulk canopy boundary layer resistance

Bulk canopy boundary layer resistance is obtained by integrating the individual leaf

boundary layer resistance over all canopy space (the complete integrated solution is given in Appendix A), and expressed as follows:

$$\bar{r}_b^{-1} = \bar{c} u_2^{1/2}. \tag{66}$$

5.3.3 Surface resistance

The formulation of stomatal resistance is taken directly from the SiB and SSiB formulations (Sellers et al., 1986; Xue et al., 1991), and is rewritten as follows

$$\bar{r}_c^{-1} = \frac{N_c}{K \cdot c}\left\{\frac{b}{f \cdot F_\pi(0)} \ln\left[\frac{\mu f e^{KLAI} + G(\mu)}{\mu f + G(\mu)}\right] - \ln\left[\frac{\mu f + G(\mu) e^{-KLAI}}{\mu f + G(\mu)}\right]\right\} F(\sum) \tag{67a}$$

for daytime, and

$$\bar{r}_c^{-1} = N_c \frac{0.5LAI}{a/b + c} F(\sum) \tag{67b}$$

for nighttime, where $f = \dfrac{a + bc}{cF_\pi(0)}$, N_c is the greenness of vegetation, a, b and c are species dependent PAR response constant, $F_\pi(0)$ PAR flux above the canopy, here K the extinction coefficient, μ the cosine of the PAR flux zenith angle, $G(\mu)$ the leaf angle projection in direction μ, and $F(\sum)$ the environmental stresses [the details can be found in Sellers et al. (1986) and Xue et al. (1991)].

The soil surface resistance is taken directly from Sellers et al. (1992), and given by

$$r_{soil} = \begin{cases} \exp(8.206 - 4.255\overline{\theta_l}^{nsoil} / \overline{\theta_{l,sat}}^{nsoil}), & \text{for soil} \\ 0, & \text{for snow} \end{cases} \tag{68}$$

5.3.4 Grid-averaged sensible heat and evapotranspiration fluxes

If there coexist bare soil, snow cover and vegetation within grid square, the bulk sensible heat and evapotranspiration fluxes are taken into account. As by an area weighed average method in our model, the bulk fluxes are given by

$$\bar{H} = H_{gb} + H_{ac}, \tag{69}$$

$$\bar{E} = E_{gb} + E_{ac}. \tag{70}$$

VI. MODEL PARAMETERS AND NUMERICAL IMPLEMENTATION

6.1 *Model Parameters*

The parameters can be divided into two categories: the primary parameters describing the nature of land surface, i.e., the dominant soil texture types, soil color types, and vegetation types within model mesh; the secondary parameters associated with the primary parameters (listed in Table 2). For AGCM applications, currently, the former's classification and geographic distribution dataset are inferred from the soil archives of BATS (Dickinson et al., 1986), and the vegetation archives of SiB (Doraman and Sellers, 1989), but with partial modification to China region by using the dataset obtained in Chinese literatures; the latter's are obtained from above model and other scientific literatures.

6.2 *Numerical Implementation of Model*

In practice, the soil column is discretized into three layers with thickness, Δz_3, Δz_2 and

Δz_1, i.e., (1) *surface layer* (Δz_3 = 1~2 cm), from which soil water can be directly evaporated into the atmosphere, and where the temperature undergoes a diurnal change; (2) *intermediate layer* (Δz_2 = 14.8~47 cm), where the vegetation rooting zone is but the root there may not exceed the bottom; (3) *deep layer* (Δz_1 = 1~3m), where the transfer of water is governed only by gravitational drainage and hydraulic diffusion, and the temperature there undergoes only the seasonal and annual variation. In the presence of snow on ground, when the depth of snow accumulation reaches 1 cm, the water and heat balance of snow media should be considered; otherwise, it can be combined with the surface soil layer. With accumulating or ablating, the snow layer will be subdivided or combined simultaneously at the end of each time step, the maximum number of discretization layers of snow is limited to 3.

Table 2. Soil and Vegetation Parameters Used in IAP94

Parameter	Definition
	(a) *Soil physical parameters*
γ_d	partial density of dry soil (kgm^{-3})
ρ_d	intrinsic density of soil (kgm^{-3})
K_{sat}	soil hydraulic conductivity at saturation (ms^{-1})
ψ_{sat}	soil water potential at saturation (m)
B	slope of the retention curve of soil water
c_d	specific heat of dry soil ($Jkg^{-1}K^{-1}$)
q_{tz}	content of quartz in soil
α_{sat}	soil surface albedo at saturation
α_{dry}	soil surface albedo at dry situation
	(b) *Vegetation morphological and physiological parameters*
F_{veg}	fraction of vegetation cover
LAI	total leaf-area index (m^2m^{-2})
N_c	canopy greenness index
wid	inverse square root of leaf dimension ($m^{-1/2}$)
z_2, z_1	height of canopy top and bottom respectively (m)
T_0, T_H, T_L	optimum, maximum and minimum temperature for stomatal functioning (K)
χ_l	Ross function of leaf-angle distribution
a, b, c, c_1, c_2	leaf stomatal resistance coefficients used in SiB and SSiB
α_A, δ_A	leaf reflectance and transmittance
c_d	leaf drag coefficient
D_1, D_2, D_3	thickness of surface, intermediate and deep soil layer (m)
$root$	fractional factor of root in soil

The sequence of calculations carried out by our model is conceptually outlined as follows:

1. Read in soil and vegetation parameters (listed in Table 2)

2. Read in initial canopy, snowpack and soil element values of temperature, thickness, water content

(a) Read meteorological data

(b) Initialize partial densities, fractions of grid cover, snow age and grain size; set water flow as zero; calculate resistances presented in Section 5

BEGIN TIME LOOP

3. Adjust the fractions of ground cover using (40), (41)

4. Read meteorological data

5. If precipitation occurs,

(a) Calculate the temperature of precipitation, formulation of wet-bulb potential temperature is used

(b) Calculate the canopy interception by using (19), (20)

(c) Calculate water flow, snow accumulation and surface runoff at the ground surface by using (24), (25). In the case of snowfall, snowfall density of 80 kgm^{-3} for air temperature greater than $-15°C$ and 50 kgm^{-3} for air temperature less than $-15°C$

(d) Calculate canopy water store and water content of top ground layer resulting from precipitation

(e) If there is no snow layer isolated from surface soil layer before this time step, and snow accumulation reaches 1 cm resulting from snowfall, add a new snow layer, and initialize the new snow temperature, partial densities and grain size

6. Determine compaction rate of snow cover by using (38), adjust thickness of snow layers, renew snow partial densities and grain sizes

7. Calculate thermal parameters, including effective thermal conductivity, combined specific heat by using (14), (17), (18)

8. Estimate albedo and transitivity of canopy, ground albedo, and the net absorbed solar radiation fluxes

9. Solve linear thermal balance equations, using tridiagonal matrix algorithm, note that they are first linearized and the differentials are approximated by discrete intervals

10. Calculate turbulent flux as following procedure:

(a) Estimate surface roughness, zero-plane displacement, and wind profile relationship by using (52) – (60)

(b) Calculate resistance $r_{ag}, r_{soil}, \bar{r}_b, r_d$

(c) Solve vapor and heat balance equations (7) and (13), $\bar{r}_c, r_{ac}, r_{gc}, T_{ac}, q_{ac}$ by using iteration method

(d) Estimate turbulent fluxes and net absorbed radiation using new temperature and humidity

11. Renew water content due to evapotranspiration as following procedures:

(a) Calculate ice sublimation, melting and water vapor diffusion within canopy, snowpack and soil

(b) Adjust water content of canopy, snowpack and soil resulting from evapotranspiration and melting

(c) Solve linear hydraulic diffusive equations for snow and soil, using tridiagonal matrix algorithm (note that they are first linearized and the differentials are approximated by discrete intervals)

(d) Renew partial densities of snow and soil layers

14. Divide or combine thick or thin snow elements (note that the thickness of surface layer is limited in the range 1cm – 2cm, and the number of snow layers is variable)

15. Save the past values of mass, thermal parameters and variables for next time step use

16. Return item 3, begin next time step.

END MAIN TIME LOOP

It should be mentioned that the prognostic equations of water balances are only considered for the liquid water constituents' [e.g., Eq.(9)] in above procedure. For other water constituents', they are treated as diagnostic formulations.

VII. EVALUATION OF THE MODEL PERFORMANCE

In this section we use several field datasets to evaluate IAP94 described above. We also compare with the other schemes. The aim of the IAP94 is not only to reasonably describe the land-surface physical processes for a particular location, but rather to have better performance of the scheme in different climate regions on global land. For this propose, we conduct a series of off-line experiments, which involve a wide range such as tropical forest, grass land, crop field, arid bare soil, frigid bare soil, and snow cover. In this paper, three experiments are presented, in which CRREL, ARME, and HAPEX-MOBILHY observational datasets are used. Here CRREL data come from CRREL snow field experiment (Cold Regions Research Engineering Laboratory, Hanover, New Hampshire; Jordan, 1986; 1989; 1990), ARME data come from central Amazonia rainforest experiment (Shuttleworth et al., 1984), and HAPEX-MOBILHY data come from HAPEX agricultural crop field experiment at Caumont in France. The last experiment is a PILPS experiment of phase 2. [Note: we also conducted the PILPS Cabauw experiment, the results of which can be found in Chen et al., (1995), and other experiments conducted by IAP94 can be found in Dai (1995)].

7.1 *CRREL*

CRREL snow-field site is located in Hanover, NH (49.6°N; 72.0°W). The forcing meteorological data used in this study are taken from the observations covering the period of 5-18 February 1987, where the observational height is 2 m above ground. The hourly observations of air temperature, wind speed, relative humidity, incident solar radiation, incident long wave radiation and precipitation rate are used. The initial snow depth is 0.55 m. When integrating IAP94, the initial data, snow and soil parameters are the same as those used in SNTHERM.89 (Jordan, 1991). For verification, the results of SNTHERM.89 are used. SNTHERM.89 has a very fine and comprehensive description for snow, which has been extensively used in snow hydrology community, but is not feasible for climate study because it is computationally demanding.

Fig.3(a, b, c) shows predicted time series by SNTHERM.89 and IAP94 for the absorbed radiation $\overline{R}_{net}$, sensible heat $\overline{H}$, latent heat $L_l\overline{E}$. The predicted fluxes by the two models agree reasonably well. Fig.3(d, e) shows predicted time evolutions of the surface temperature and snow thickness by SNTHERM.89 and IAP94. In surface temperature simulated by IAP94, the crest values are slightly lower than by SNTHERM.89 (approximately 0.5 – 1 K). These differences seem to be caused by the prescription of minimum thickness of surface layer. In IAP94, the minimum thickness is limited at 1.0 cm, but that in SNTHERM.89 is at 0.2 cm. The heat capacity for SNTHERM.89 is larger, and needs more heat to reach the crest temperature. The total snow thickness simulated by IAP94 is somewhat thicker than that by SNTHERM.89, since the prescribed maximum number of snow layer in IAP94 is 3, and less than that in SNTHERM.89, and the underlying layers load less weight from the tops, and then underestimate the pressure metamorphism.

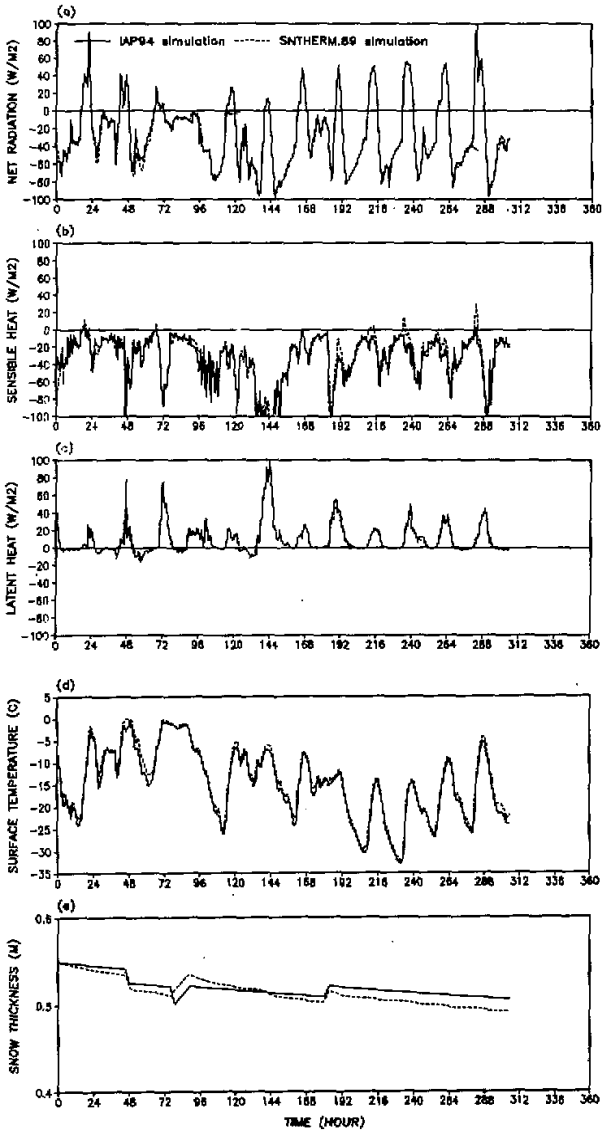

Fig. 3. Daily variations of IAP94 and SNTHERM.89 predicted (a) net radiation, (b) sensible heat flux, (c) latent heat flux, (d) surface temperature, and (e) snow depth at a snowfield (CRREL, Hanover, New Hampshire, USA, 5–18 February.

7.2 *ARME*

The ARME site is located in the central Amazonia, Brazil, and was selected as representative of rainforest. The forcing meteorological data and the verifying fluxes data used in this study are taken from the observations covering the period of 1–30 September 1983 on a tower

at a height of 45m, approximately 10m above the forest canopy. The hourly observations of wind, temperature, humidity, rainfall, radiation, and fluxes of sensible and latent heat are used. When integrating IAP94, the initial data, vegetation and soil limit are the same as those used in Xue et al. (1991), Sellers and Dorman (1987).

Fig.4(a, b, c) shows the observed and predicted time series by SSiB and IAP94 for the absorbed radiation $\overline{R}_{net}$, sensible heat $\overline{H}$, latent heat $L_v\overline{E}$. The predicted fluxes by IAP94 and the observations are generally in good agreement. Comparing the results of SSiB, we find that the net radiation predicted by two models are very close to observational values, but there is a slight discrepancy in sensible and latent heat fluxes. SSiB reproduces a somewhat higher sensible heat and lower latent heat than IAP94, and IAP94's are relatively more close to the observations in most of the days.

Fig.4(d, e, f) shows SSiB and IAP94 predicted time evolutions of canopy temperature T_c, soil surface temperature T_{nsoil}, and total soil water content (in total 3.5m). The IAP94 and SSiB predicted values generally agree well. The differences are the surface soil temperature and soil moisture simulations. Except the period from 6 September to 9 September, the crest values of surface soil temperature simulated by IAP94 are somewhat lower than SSiB's, and a time-lag covers all the integrating days. Additionally, relative to SSiB's, a decrease tendency of the total soil water exists, which starts from 20 September.

7.3 HAPEX-MOBILHY

This experiment exactly follows the PILPS HAPEX experiment in phase 2(b). The data and experimental design can be found in Shao et al. (1994) in detail. Two experiments are conducted in our present study, one is the control experiment (PILPS HAPEX Experiment 1), in which the forcing meteorological data and parameters for charactering land surface properties are from the observations of HAPEX MOBILHY; the other is one of the improved control experiment (PILPS HAPEX Experiment 13), in which a new set of soil hydrological parameters are used. Since the major objectives of PILPS HAPEX experiment are to assess soil moisture simulation in PILPS schemes, only the results of soil moisture simulation are presented in this paper, and the other results, such as fluxes, temperature and runoff, can be found in Dai (1995).

Fig.5(a) shows the observed and predicted by IAP94 annual cycle of total soil water. There is a general agreement between the simulation and observation. IAP94 correctly describes the annual trend of soil moisture in a qualitative sense: soil remains wet for the first four months of the year with soil moisture close to the field capacity, soil water depletes at the beginning of the growing season (early May), the soil is driest between August and October, and becomes increasingly wet after October. In the control experiment, except that soil water for the growing season is slightly under-predicted, the simulation by IAP94 agrees fairly well with observations. In Experiment 13, IAP94 underestimates soil moisture for most times of year, especially for the growing season. The results are similar to PILPS schemes (Shao et al., 1994).

Fig.5(b) shows the observed and predicted by IAP94 annual cycle of the soil moisture in the root zone. In contrast to total soil water content, the results for Experiment 13 agree reasonably well with observations, however, for the control experiment, IAP94 underestimates soil moisture for most times of year, especially for the growing season.

Fig.5(c) shows the observed and predicted by IAP94 annual cycle the soil moisture in top 0.1m. The results are similar to the root zone case. Comparing with PILPS schemes' (Shao et al., 1994), IAP94 is of a good performance in this experiment.

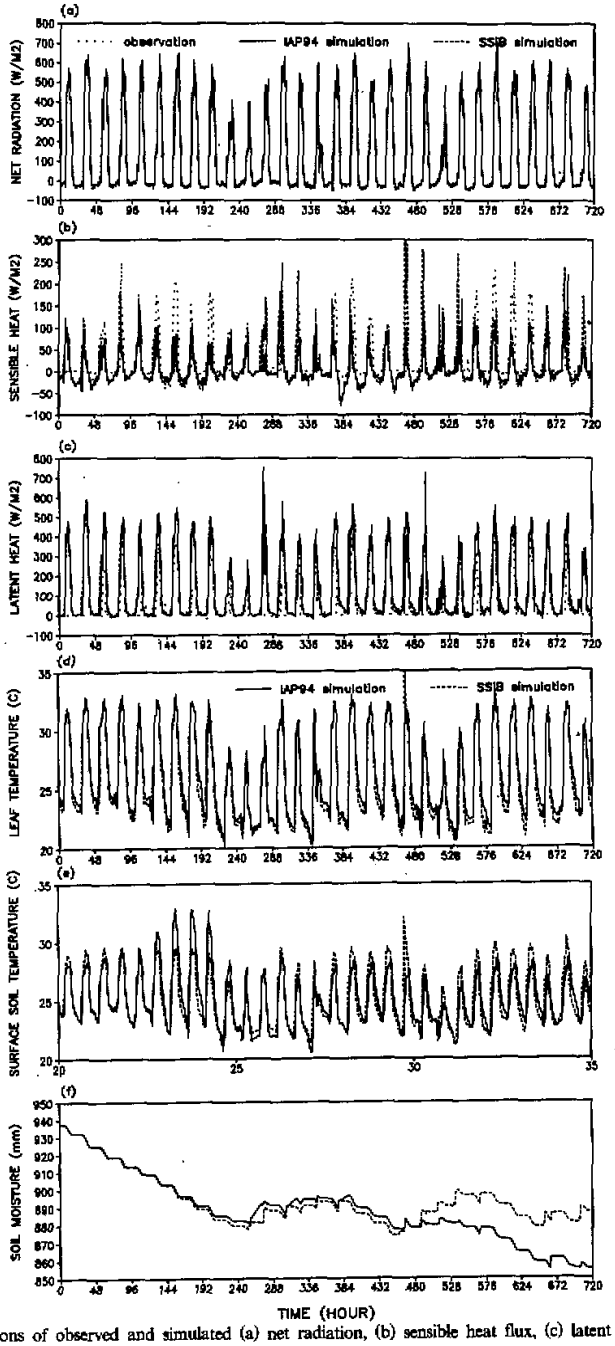

Fig. 4. Daily variations of observed and simulated (a) net radiation, (b) sensible heat flux, (c) latent heat flux, (d) leaf temperature, (e) soil surface temperature, and (f) soil water content (total 3.5 m) at a rain-forest site (Central Amazon basin, Brazil, 1-30 September, 1983).

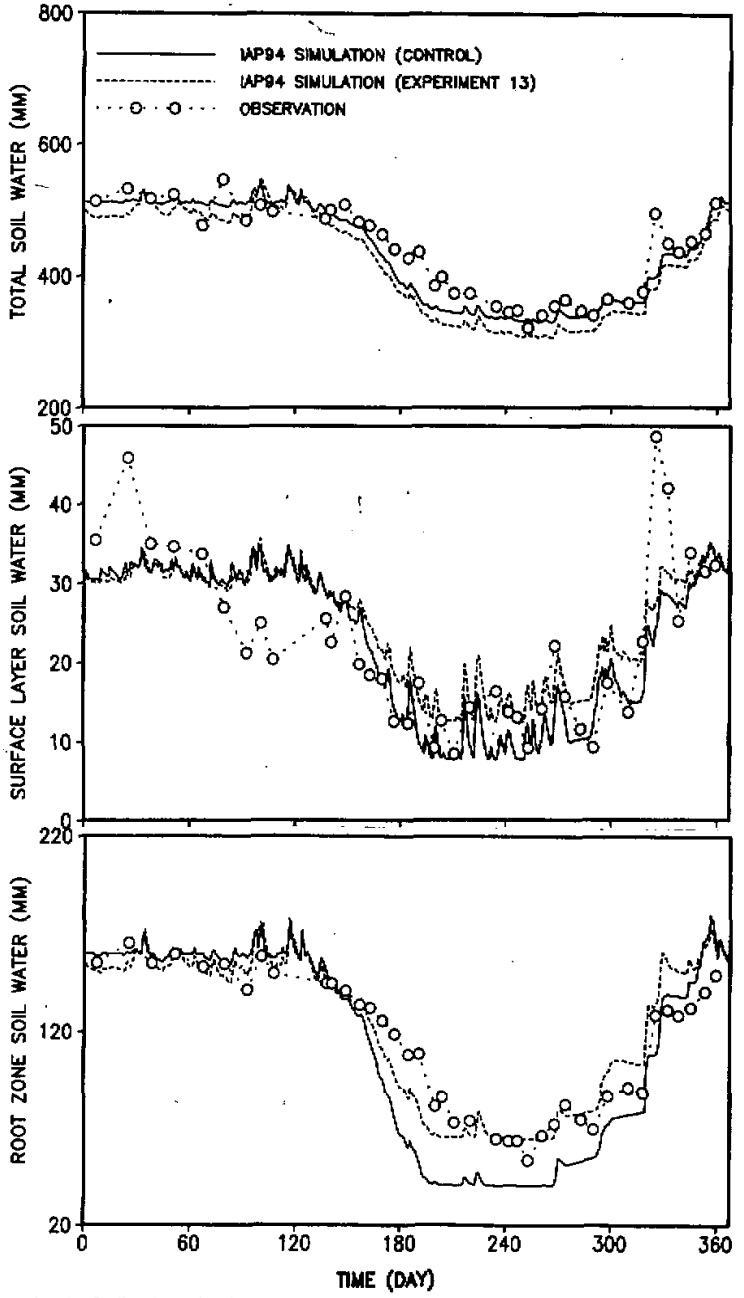

Fig. 5. Annual cycle of soil moisture (mm) for three layers as simulated by IAP94 compared with HAPEX data, (a) total 1.6 m, (b) top 0.5 m, and (c) top 0.1 m. The observation data are shown for HAPEX weekly measurements for respective layers (closed circles). The simulated results are shown for two runs (PILPS HAPEX Experiment 1–control, PILPS HAPEX Experiment 13).

VIII. SUMMARY AND CONCLUSIONS

The IAP (Institute of Atmospheric Physics, Chinese Academy of Sciences) land-surface model (IAP94) for use within GCMs has been described in detail. The scheme has been tested against field measurements, and compared with the SNTHERM.89 (Jordan, 1991) and SSiB (Xue et al., 1991), corresponding to a wide range of surface conditions and meteorological forcing.

This scheme is comprehensive to some extent and is suitable for different surface types of all global landscape. In its development, IAP94 has emphasized the substantial physical basis, and included all primary factors as comprehensive as possible, additionally, stressed the efficient and economical numerical computational schemes.

Based on the mixture theory (Morland et al., 1990) and the theory of porous media fluid dynamics (Bear, 1972), the system of conservational equations for water and heat of soil, snow and vegetation canopy has been constructed. All factors that may affect the water and heat balance in media can be considered naturally, and each factor and term possess a distinct physical meaning. In the computation of water content and temperature, the water phase change and the heat transported by water flow were taken into account, namely, a coupled treatment for all these factors has been carried out partly. The difficult treatment for water phase change becomes more convenient in IAP94. Moreover, a particular attention has been paid to the water vapor diffusion in soil in arid or semi-arid regions, and snow compaction in IAP94. The effect of the difference between aerodynamic roughness and thermal roughness on the surface turbulent transfer was taken into account as well. The aerodynamic roughness of vegetation is a function of canopy density, height and zero-plane displacement. An extrapolation of log-linear and exponential relationship is used in describing the wind profile within canopy. IAP94 consists of a large number of linked process schemes, some of them are cited from the scientific literatures.

In conclusion, IAP94 seems to be able to capture the main physical mechanisms governing the land-surface processes. But many approaches towards the improvements remain opened, for example, the parameterizations for overland runoff and lateral ground-water flow, particularly when topographic forcing is considered. A detailed check and sensitive tests over the vegetation and soil characteristics, such as stomatal resistance, roughness, wind profile relationship, snow masking effects in albedo, soil heat capacity and conductivity, will be conducted in the future. Finally, some methods to improve the modelling of subgrid-scale variability of convective precipitation, surface soil moisture and grid averaged surface fluxes may have to be sought, perhaps along the lines of the work of Avissar et al. (1989) and Noilhan et al. (1995). In order to verify those aspects of the model formulation, the GEWEX provides a fruitful dataset at different scales to test the performance in off-line cases and assumptions related to spatial averaging at a grid scale. The results of these numerical experiments will be presented in the forthcoming papers.

The authors wish to thank Dr. Rachel Jordan for kindly providing SNTHERM.89 document and codes and for her useful suggestions, and Dr. Yong-Kang Xue for providing SSiB and his many generous helps. We are grateful to Dr. Tian-Hong Chen and the others of the PILPS team for their valiant and tireless efforts in PILPS experiment. We would like to extend our gratitude to all the people who provided us the field measurement data. The very constructive comments of Dr. Sam Chang, Zong-Liang Yang, Sam Yee, Don Norquist, Xiao-Ping Zhou were also greatly appreciated.

Appendix A

Bulk boundary layer resistance coefficient $\bar{r}_b$

The individual leaf boundary resistance was given by Goudriaan (1977) as

$$r_{b,h} = 90 \times (u \cdot wid)^{-1/2}. \tag{A1}$$

Here u is the wind speed over the leaf surface (ms^{-1}), and wid the inverse square root of leaf dimension ($m^{-1/2}$). Assuming the exponent-line part is dominant in wind profile within canopy, and integrating (59), we can obtain $\bar{r}_b$ as follows

$$\bar{r}_b^{-1} = \int_0^{LAI} r_{b,h}^{-1} dL = \bar{c} u_2^{1/2}, \tag{A2}$$

where

$$\bar{c} = (90 wid^{1/2})^{-1} \frac{LAI}{z_2 - z_1} \frac{4k^2 z_2}{c_{*1}} \bar{c}'$$

$$\bar{c}' = f^{1/2} \left\{ 1 - \exp\left[-\frac{c_{*1}}{4k^2} \left(1 - \frac{z_1}{z_2} \right) \right] \right\} + (1-f) f^{-1/2} \exp\left(\frac{c_{*1}}{4k^2} \right) \left(\frac{1}{\ln(z_2 / z_{GM})} \times \right.$$

$$\left. \left\{ \left[\ln(z_2 / z_{GM}) \exp\left(\frac{c_{*1}}{4k^2} \right) - \ln(z_1 / z_{GM}) \exp\left(\frac{c_{*1} z_1}{4k^2 z_2} \right) \right] - \left[\ln(z_2 / z_1) + \frac{c_{*1}(z_2 - z_1)}{4k^2 z_2} \right] \right\} \right.$$

Appendix B

Spatial discretization formulation of water fluxes within soil and snow

In spatial discretizing, the central-difference method is used. The discretization formulations of (26), (30) and (33) are given by:

(a). Water flux from soil layer j to soil layer $j+1$

$$U_l^{j+1/2} = -\rho_l K_{sat} \left(\frac{\overline{\theta_l}^{j+1} + \overline{\theta_l}^{j}}{\overline{\theta_{l,sat}}^{j+1} + \overline{\theta_{l,sat}}^{j}} \right)^{2B+3}$$

$$\times \left[1 - \frac{2\psi_{sat} B}{\left(\overline{\theta_{l,sat}}^{j+1} + \overline{\theta_{l,sat}}^{j} \right)} \left(\frac{\overline{\theta_{l,sat}}^{j+1} + \overline{\theta_{l,sat}}^{j}}{\overline{\theta_l}^{j+1} + \overline{\theta_l}^{j}} \right)^{B+1} \left(\frac{\overline{\theta_l}^{j+1} - \overline{\theta_l}^{j}}{\Delta z_{j+1} + \Delta z_j} \right) \right] \tag{B1}$$

(b). Water flux from snow layer j to snow layer $j+1$

$$U_l^{j+1/2} = -K_{max} \frac{\rho_l^2 g}{\mu_l} \left(\frac{s_e^{j+1} + s_e^{j}}{2} \right)^3 \tag{B2}$$

(c). Water-vapor flux from soil layer j to soil layer $j+1$

$$U_v^{j+1/2} = -(\overline{D_v C_\theta}^{j+1} + \overline{D_v C_\theta}^{j}) \left(\frac{\overline{\theta_l}^{j+1} - \overline{\theta_l}^{j}}{\Delta z_{j+1} + \Delta z_j} \right) \tag{B3}$$

REFERENCES

Anderson EA (1976), A point energy ad mass balance model of a snow cover, Office of Hydrology, National Weather Service Silver Spring, Maryland, NOAA Technical Report NWS 19.

Avissar R, Pielke RA (1989), A parameterization of heterogeneous lad surfaces for atmospheric general numerical

models and its impact on regional meteorology, *Mon. Wea. Rev.*, **117**: 2113–2136.

Bear J (1972), *Dynamics of fluids in porous media*, American Elsevier, New York. 764pp.

Bhumralkar CM (1975), Numerical experiments on the computation of ground surface temperature in atmospheric circulation model, *J. Appl. Meteor.*, **14**: 1246–1258.

Brutsaert W (1979), Heat and mass transfer to and from surfaces with dense vegetation or similar permeable roughness, *Boundary-Layer Meteor.*, **16**: 365–388.

Chen F, Janjic Z, Mitchell K (1996), Impact of atmospheric surface layer parameterization in the new land-surface scheme of the NCEP mesoscale eta numerical model (submitted to Boundary-Layer Meteor.).

Chen TH, coauthors (1997), Cabauw experimental results from the Project for intercomparison of Land-Surface Parameterization Schemes (PILPS), *J. Climate*[1] (in press).

Clapp R, Hornberger G (1978), Empirical equations for some soil hydraulic properties, *Water Resource Research*, **14**: 601–604.

Colbeck SC (1971), A theory of water percolation in snow, *J. Glaciology*, **11(63)**: 369–385.

Dai Yongjiu (1995), A land surface model for AGCMs and its coupling with IAP two-level AGCM, Ph.D thesis, Institute of Atmospheric Physics, Chinese Academy of Sciences, 320pp (in Chinese).

Dickinson RE (1988), The force-restore model for surface temperatures and its generalizations, *J. Climate*, **1**: 1086–1097.

Dickinson RE, A Henderson-Sellers, Kennedy PJ, Wilson MF (1986), Biosphere atmosphere transfer scheme (BATS) for NCAR Community Climate Model, NCAR Tech. Note NCAR / TN-275+STR, 69pp.

Dickinson RE, A Henderson-Sellers, Kennedy PJ, Wilson MF (1993), Biosphere atmosphere transfer scheme (BATS) version 1e as coupled to for Community Climate Model, NCAR Tech. Note NCAR / TN-378+STR, 72pp.

Dorman JL, Sellers PJ (1989), A global climatology of albedo, roughness length and stomatal resistance for atmospheric general circulation models as represented by the simple biosphere model (SiB), *J. Appl. Meteor.*, **28**: 833–855.

Dyer AJ (1974), A review of flux-profile relations, *Boundary Layer Meteor.*, **1**: 363–372.

Farouki OT (1981), Thermal properties of soil, USA Cold Regions Research & Engineering Laboratory, CRREL Monograph 81-1, 136pp.

Garratt JR (1992), *The Atmospheric Boundary Layer*, Cambridge University Press, 316pp.

Garratt JR (1993), Sensitivity of climate simulations to land-surface and atmospheric boundary-layer treatments – A review, *J. Climatology*, **6**: 419–449.

Gates WL, A Henderson-Sellers, Boer GJ, Folland CK, Kitoh A, McAvaney BJ, Semazzi F, Smith N, Weaver AJ, Zeng QC (1996), Climate models-Evaluation, in *IPCC Second Scientific Assessment of Climate Change*, Cambridge University Press.

Goudriaan J (1977), Crop Micrometeorology: A simulation study, Wageningen Center for Agricultural Publishing and Documentation, 249pp.

Haynes FD, Carbee DL, VanPelt DJ (1980), Thermal diffusivity of frozen soil, USA Cold Regions Research and Engineering Laboratory, Special Report 80-38, 30pp.

Henderson-Sellers A, Wilson MF, Thomas G, Dickinson RE (1986), Current global land-surface data sets for use in climate-related studies, NCAR Technical Note NCAR / TN-272+STR, 110pp.

Inoue E (1963), On the turbulent structure of airflow within crop canopies, *J. Meteor. Soc. Japan*, **41**: 317–326.

Jordan R.(1991), A one-dimensional temperature model for a snow cover: Technical documentation for SNTHERM. 89. USA Cold Regions Research and Engineering Laboratory, Special Report 91-16, 49pp.

Jordan R., O'Brien, Bates RE (1986), Thermal measurements in snow, *Proceedings of snow symposium V. USA Cold Regions Research and Engineering Laboratory*, Special Report 86-15.

Kimball BA, Jackson RD, Nakayama FS, Idso SB, Reginato RJ (1976), Soil-heat flux determination: Temperature gradient method with computed thermal conductivities, *Soil Sci. Soc. Am. J*, **40**: 25–28.

Kondo J, Saigusa N (1992), A model and experimental study of evaporation from bare-soil surface, *J. Appl. Meteor.*, **31:** 304-312.

Kondo J, Saigusa N, Sato T (1990), A parameterization of evaporation from bare soil surfaces, *J. Appl. Meteor.*, **29:** 383-387.

Kondratyev K Ya, Korzov VI, Mukhenberg VV, Dyachenko LN (1981), The shortwave albedo and the surface emissivity, *Land surface processes in Atmospheric General Circulation Models*, P.S. Eagleson, Ed., Cambridge University Press, 463-503.

Louis JF (1979), A parametric model of vertical eddy fluxes in the atmosphere, *Boundary Layer Meteor.*, **17:** 187-202.

Louis JF, Tiedtke M, Geleyn JF (1982), A short history of the PBL parameterization at ECMWF, *Proceedings, ECMWF workshop on planetary boundary layer parameterization*, Reading, 25-27 Nov. 81, 59-80.

Mahrt L (1987), Grid-averaged surface fluxes, *Mon. Wea. Rev.*, **115:** 1550-1560.

Mehta BK, Shiozwa S, Nakano M (1994), Hydraulic properties of sandy soil at low water contents, *Soil Science*, **157(4):** 208-214.

Milly PCD, Eagleson PS (1984), Parameterization of moisture and heat fluxes across the land surface for use in atmospheric general circulation models, Rep. 279, Dept. of Engineering, MIT, 159 pp.

Morland LW, Kelly RJ, Morris EM (1990), A mixture theory for a phase-changing snowpack, *Cold Reg. Sci. and Tech.*, **17:** 271-285.

Noihan J, Lacarrere P (1995), GCM grid-scale evaporation from mesoscale modelling, *J. Climate*, **8:** 206-223.

Patankar SV (1980), *Numerical heat transfer and fluid flow*, New York, Hemisphere Publishing.

Philip J (1957), Evaporation, and moisture and heat fields in the soil, *J. Meteor.*, **14:** 354-366.

Sellers PJ (1985), Canopy reflectance, photosynthesis and transpiration, *Int J. Remote Sens.*, **8:** 1335-1372.

Sellers PJ, Mintz Y, Sud YC, Dalcher A (1986), A simple biosphere model (SiB) for use within general circulation models, *J. Atmos. Sci.*, **43:** 505-531.

Sellers PJ, Heiser MD, Hall FG (1992), Relationship between surface conductance and spectral vegetation indices at intermediate (100 m^2- 15m^2) length scales, *J. Geophys. Res., FIFE Special Issue*, **97:** 19033-19060.

Sellers PJ, Randall DA, Collatz GJ, Berry JA, Field CB, Dazlich DA, Zhang C, Collelo GD, Bounoua L (1996), A revised land surface parameterization (SiB2) for atmospheric GCMs, Part I: Model formulation, *J. Climatology*, **9:** 676-705.

Shao YP, coauthors (1994), Soil moisture simulation: A report of the RICE and PILPS workwhop, GEWEX / GAIM Rep., IGPO Publication Series, No. 14, 179 pp.

Shuttleworth WJ, coauthors (1984), Eddy correction measurements of energy partition for Amazonian forest, *Quart. J. Roy. Meteor. Soc.*, **110:** 1143-1162.

Verseghy DL (1991), CLASS - a Canadian land surface scheme for GCMs, 1. soil model, *Int. J. Climatol.*, **11:** 111-133.

Verseghy DL, McFarlane NA, Lazare M (1993), CLASS - a Canadian land surface scheme for GCMs, 2. vegetation model and coupled runs, *Int J. Climatol.*, **13:** 347-370.

Viterbo P, Beljaars ACM (1995), An improved land surface parameterization scheme in the ECMWF model and its validation, *J. Climatology*, **8:** 2716-2748.

Xue YK, Sellers PJ, Kinter JL, Shukla J (1991), A simplified biosphere model for global climate studies, *J. Climatology*, **4:** 345-364.

Yamazaki T, Kondo J, Watanabe T (1992), A heat-balance model with a canopy of one or two layers and its application to field experiments, *J. Appl. Meteor.*, **31:** 86-103.

Yen Y (1981), Review of thermal properties of snow, ice and sea-ice, CRREL Rep, 81-10.